Scavenging free iron reduces arteriolar microvasospasms after experimental subarachnoid hemorrhage

Hanhan Liu MD[1*], Julian Schwarting MD[1,2*], Nicole Angela Terpolilli MD[1,2,3], Kathrin Nehrkorn PhD[1,3], and Nikolaus Plesnila MD, PhD[1,3]

[1] Institute for Stroke and Dementia Research, [2] Department of Neurosurgery, University of Munich Medical Center, Ludwig-Maximilians-University (LMU), and [3] Munich Cluster of Systems Neurology (Synergy), Munich, Germany.

*These authors contributed equally to this work

Running title:

Iron induces microvasospasms after experimental SAH

Correspondence to:

Nikolaus Plesnila, MD, PhD, Institute for Stroke and Dementia Research, University Hospital, LMU Munich, Feodor-Lynen Strasse 17, 81377 Munich, Germany. E-mail: nikolaus.plesnila@med.uni-muenchen.de

Abstract:

Background and Purpose

Subarachnoid hemorrhage (SAH) is associated with acute and delayed cerebral ischemia resulting in high acute mortality and severe chronic neurological deficits. Spasms of the pial and intraparenchymal microcirculation (microvasospasms, MVS) contribute to acute cerebral ischemia after SAH, however, the underlying mechanisms remain unknown. We hypothesize that free iron (Fe^{3+}) released from hemolytic red blood cells into the subarachnoid space may be involved in MVS formation.

Methods

Male C57BL/6 mice (n=8/group) received 200 mg/kg of the iron scavenger Deferoxamine (DFX) or vehicle i.v. and were then subjected to SAH by filament perforation. MVS of pial and intraparenchymal vessels were imaged three hours after SAH by *in vivo* 2-photon microscopy.

Results

MVS occurred in all investigated vessel categories down to the capillary level. DFX significantly reduced the number of MVS after experimental SAH. The effect was almost exclusively observed in larger pial arterioles (>30 µm) covered with blood.

Conclusion

These results provide proof-of-principle evidence that Fe^{3+} is involved in the formation of arteriolar MVS after SAH and that arteriolar and capillary spasms are triggered by different mechanisms. Deciphering the mechanisms of Fe^{3+}-induced MVS formation may result in novel therapeutic strategies for SAH patients.

Keywords: subarachnoid hemorrhage, microvasospasm, iron, deferoxamine

Introduction

Subarachnoid hemorrhage (SAH) is a devastating subtype of stroke with a high pre- (20-25%) and in-hospital mortality (18% to 30%).[1] SAH is mainly caused by rupture of intracranial aneurysms (85%) and occurs in younger patients than ischemic stroke (40–60 years of age). Despite recent improvements of emergency medicine and surgical treatments, mortality and morbidity remain high after SAH and therapeutic options are limited and mostly restricted to symptomatic treatment. Mechanisms of post-hemorrhagic brain damage remain unclear and are therefore not amenable to specific therapeutic strategies.[2]

The rupture of an intracranial aneurysm and the subsequently evolving hematoma cause an abrupt rise of intracranial pressure (ICP), a decrease of cerebral perfusion pressure (CPP), which may thus decrease cerebral blood flow (CBF) and result in global cerebral ischemia. ICP usually peaks in the first few minutes after hemorrhage and then quickly decreases. Cerebral perfusion, however, remains impaired beyond the acute phase causing secondary ischemic

changes.[3, 4] These changes occur within the first hours and days after SAH, but may also occur with a delay of more than one week after hemorrhage. For decades, delayed vasospasms of large pial arteries mediated by the ET_A endothelin receptor subtype were believed to be mainly responsible for poor outcome after SAH.[5, 6] However, clinical trials investigating the effect of the specific ET_A inhibitor Clazosentan after SAH, demonstrated a reduction of clinically detectable macrovasospasms, but no improvement of patient outcome.[7] These findings resulted in a reevaluation of the pathophysiology of cerebral ischemia after SAH and it was recognized that microcirculatory dysfunction may also play an important role for the development of post-hemorrhagic cerebral ischemia and subsequent brain damage.[5, 7-9] A variety of pathological phenomena first described in experimental animals by histology and later observed *in vivo* and validated in patients, were shown to occur in the cerebral microcirculation after SAH, such as microthrombosis, vascular inflammation, endothelial dysfunction, and spasms of pial and intraparenchymal arterioles.[10 11, 12 19] As a consequence, parenchymal perfusion decreased[9] and local ischemia resulted in lipid peroxidation and tissue damage.[16,18] So far, however, the mechanisms underlying the formation of cerebral microvasospasm have not been elucidated. Recent studies imply that endothelial dysfunction may play a significant role.[13]

Nitric oxide (NO) is involved in the regulation of physiological cerebral blood flow and the proper function of neurovascular coupling and lack of NO is one of the main mechanisms of endothelial dysfunction. After SAH, NO levels rapidly decrease and exogenous supply of NO significantly reduces MVS,[14] suggesting a key role for NO in the pathogenesis of microvasospasm formation. However, the mechanisms causing NO depletion in the microvasculature after SAH remain unclear. A potential link between the blood present in the subarachnoid space after SAH and endothelial NO depletion could be iron (Fe)-mediated formation of reactive oxygen species (ROS) in the perivascular space. ROS are very effective NO scavengers and could thus explain microvascular dysfunction after SAH.[15]

Following SAH, lysis of erythrocytes and degradation of hemoglobin (Hb) release large amounts of free iron (Fe^{3+}) into the subarachnoid space.[16] Previous studies have also suggested a contribution of iron for brain injury after SAH,[17] however, whether this effect is mediated by spams of the cerebral microcirculation has not been evaluated so far. We therefore hypothesize that microvasospasms after subarachnoid hemorrhage are caused by free iron in the subarachnoid space. In order to prove this hypothesis, we injected the iron chelator Deferoxamine (DFX) into the systemic circulation of mice before SAH and observed the cerebral microcirculation three hours later by *in vivo* 2-photon microscopy. This approach allowed us to make sure that DFX extravasates together with blood into the subarachnoid space after induction of hemorrhage and reaches at defined and

sufficiently high concentration the desired site of action, i.e. the perivascular space of pial microvessels.

Materials and Methods

The authors declare that all supporting data are available within this article. All procedures on animal, the calculation of the sample size, and all statistical methods were reviewed and approved by the Animal Ethics Committee of the Government of Upper Bavaria (protocol number Vet_02-11-132). Sample size was calculated using SigmaPlot 12.0 (Systat Software Inc.). The results of the study are reported in accordance with the ARRIVE guidelines.[18] Given the relevant differences between sexes with respect to stroke pathophysiology and given that this study was designed as a proof-of-principle study with no therapeutic intent, we used only male animals with an age of 6 to 8 weeks and a weight of 20 to 23 gram, thereby ensuring comparability of our results with previous studies performed in our laboratory using the same experimental setup. All experiments were performed in a blinded and randomized fashion by drawing lots. Group allocation was revealed only after all experiments were performed and all data were analyzed.

Induction of subarachnoid hemorrhage

SAH was induced by endovascular perforation of the Circle of Willis in anesthetized (0.05 mg/kg fentanyl, 0.5 mg/kg medetomidine, and 5 mg/kg midazolam i.p.), intubated and artificially ventilated mice under multimodal monitoring as previously described.[19, 20] Briefly, intracranial pressure (ICP) and cerebral blood flow (CBF) were continuously monitored with an epidural probe

(Codman ICP monitor, Johnson & Johnson, UK) and with laser Doppler fluxmetry (Periflux 5000, Perimed, Sweden), respectively. A 5-0 monofilament (Prolene® 5-0, Ethicon, Germany) was inserted though the external carotid artery and advanced intracranially. Perforation of the Circle of Willis at the level of the MCA was detected via a rapid ICP increase over 50 mmHg and decline of CBF below 20% of baseline. After SAH induction, ICP and CBF were monitored for 20 minutes. SAH caused hemorrhage at the skull base and blood distributed along the branches of the MCA as demonstrated by images of perfused brains (**Figure 1A**), while sham surgery, which followed the same protocol except for MCA perforation, did not induce any bleeding (data not shown).

In vivo imaging of microvasospasms by two-photon microscopy

2-photon microscopy was performed through a thinned skull preparation as previously described.[20, 21] Briefly, mice were anaesthetized as described above, the head was immobilized using a nose clamp (David Kopf instruments, USA), and the bone above the branches of the middle cerebral artery was thinned under continuous cooling with 0.9% NaCl after local application of a 2% lidocaine solution.

In vivo imaging was performed with a Zeiss LSM 7 microscope equipped with a 20x water immersion objective (Plan Apochromat, Zeiss, Germany) and a Li:Ti laser (Chameleon, Coherent, USA). After placing the animal under the microscope, the plasma markers fluorescein isothiocyanate- (FITC) or

tetramethylrhodamine-dextran (0.5% in saline, Sigma Aldrich, USA) were injected i.v. to visualize cerebral vessels (**Figure 1B, left panel**). Dyes were excited at a wavelength of 830 nm and fluorescence was detected using band pass filters at 500-550 and/or 565-610 nm. Four regions of interest (ROI) with a size of 607 x 607 µm were imaged in 3D at a depth of 150 to 400 µm (**Figure 1B, right panel**). Line scans were performed with high frequency along pial arteries, veins, and capillaries for blood flow velocity measurements.

Experimental protocol

DFX (200 mg/kg, Desferal®, Novartis, Germany), solved in 0.9% saline, or vehicle (0.9% saline) were injected intravenously 1.5 hours prior to hemorrhage induction (**Figure 1C**). In order demonstrate that DFX or vehicle were successfully injected and reached the subarachnoid space after SAH, the injected compounds were solved with Tetramethylrhodamine (TMRM) dextran (0.5% in 0.9% NaCl). After surgical preparation, MCA perforation was performed, and anesthesia was antagonized after monitoring ICP and CBF for 20 minutes. Two hours later, animals were re-anesthetized, a femoral arterial catheter was placed for continuously measurements of arterial blood pressure and blood gas analysis, and the skull was thinned. After imaging of the four ROIs, blood samples for blood gas analysis were obtained and mice were sacrificed by transcardial perfusion with 4% PFA. Brains were removed and stored for further analysis.

Data analysis

The vessel diameter of pial and intraparenchymal vessels was analyzed as previously described.[20] Briefly, vasospasms were identified by their characteristic pearl-string like phenotype. The narrowest and the adjacent distal and proximal widest diameters were assessed, and the degree of vessel constriction was expressed in percent of the neighboring vessel segments. Vasospasm was defined as a reduction of vessel diameter larger than 15%. The number of vasospasms per individual animal was determined in a minimum of four different vessel segments.

Perfused vessel volume was assessed by counting all pixels stained with FITC dextran, extravasated blood volume was calculated by assessing pixels solely stained with TMRM dextran. Both pixel volumes were calculated by 3D reconstruction of cropped stacks (607 x 607 x 140µm) from each ROI (Imaris, Bitplane AG, Switzerland). Blood flow velocity was calculated by dividing the distance travelled by red blood cells in µm by the respective scanning time in milliseconds.

Statistical analysis

Statistical analysis was performed using GraphPad Prism 8.3 (LLC, USA). For comparison of ICP and CBF values ANOVA with Dunn´s post-hoc analysis was used for comparison between groups and ANOVA for repeated measurements with Dunnet´s post hoc test was used; values are compared to baseline measurements taken at t = 5 minutes before SAH induction. The other parameters were compared using the Man Whitney Rank Sum test. Normal distribution was tested by Shapiro-Wilk test and p-values <0.05 were regarded to indicate a statistically significant difference between groups. The Bonferroni method was used to correct for for multiple comparisons. Complete statistical data is attached in the supplementary materials.

Results

Five of 21 animals died before randomization to treatment (mortality rate 24%), ICP and CBF data of these animals was excluded from analysis. After SAH induction, ICP promptly peaked above 50 mmHg (**Figure 2A**) while regional CBF (rCBF) dropped to levels below 20% of baseline (**Figure 2B**) in both experimental groups. Within five minutes, ICP stabilized at around 20 mmHg until the end of the monitoring period, while rCBF recovered to baseline levels within 10 minutes. There were no significant differences in ICP (p = .497) or rCBF (p = .195)

between the DFX and vehicle group, indicating that SAH severity was comparable in both groups.

Physiological monitoring indicated that animals receiving DFX were slightly hypotensive and tachycardic in comparison to the control-group (**Table 1**). Since hypotension and tachycardia are well-known side effects of DFX, our measurements indicate that all animals received a pharmacologically active dose of DFX. All other recorded parameters including body temperature, blood pressure, $_{ET}pO_2$, and blood gases were within the physiological range and not different between groups (**Table 1**).

Microvasospasms were visualized three hours after SAH by *in vivo* 2-photon microscopy, as previously reported (**Figure 3**).[9, 11] Investigated subarachnoid vessels were surrounded by extravasated blood as evidence by the presence of the red plasma dye TREM in 3D reconstructed images (**Figure 3A**). These findings were corroborated by images taken from perfused brains after sacrifice of the animals (**Figure 1A**) and demonstrate that *in vivo* microscopy was performed in a vascular territory affected by hemorrhage, i.e. in a pathophysiological relevant area. After SAH, pial arterioles showed the typical pearl-string like phenotype (**Figure 3B, SAH**), while sham operated animals did not show any arteriolar spasms (data not shown).

In animals treated with DFX, no pearl-string like phenotype was observed in pial arterioles (**Figure 3B, SAH+DFX**). Quantification of images from all mice

revealed a significantly lower number of vasospasms in arterial microvessels as compared to vehicle treated mice (**Figure 4A**, **total**; p = .037). On closer examination, the number of vasospasms was only reduced in vessels covered with blood (**Figure 4A**; p = .022), while in microvessels not covered with blood DFX had no significant effect on microvasospasm formation (**Figure 4A** p = .478), suggesting that DFX acts only in areas where iron is present. When examining different vessel categories, i.e. the whole vascular tree from the capillary to the arteriolar level, we observed that DFX had no effect on capillaries and smaller arterioles, which are usually not covered with blood, while microvasospasms were completely abolished in arterioles with a diameter of 30-40 µm and in arterioles with diameters larger than 40 µm, i.e. those vessels usually covered with blood (**Figure 4B**).

In order to investigate if the prevention of microvasospasm formation in larger pial arterioles improved parenchymal perfusion, we assessed blood flow velocity of parenchymal vessels and the perfused vessel volume of arterioles and capillaries (**Figure 5**). Despite the fact that blood flow velocity was heavily reduced in all vessel territories (**Figure 5A**; normal values are indicated by the dotted lines), DFX had no effect on both investigated parameters (**Figure 5 A and B**). This observation is well in line with the fact that DFX prevented microvasospasm formation in larger, i.e. distal vessels, but had no effect on the cerebral microcirculation, which ultimately determines tissue perfusion.

Discussion

Our current results obtained by *in vivo* 2-photon imaging of pial and parenchymal cerebral vessels in a clinically relevant model of SAH in mice indicate that free iron released from blood located around subarachnoid vessels is a key mediator of arteriolar MVS after SAH. Since iron scavenging does not affect spasms of pre-capillary vessels and capillaries, our findings further indicate that arterial/arteriolar and capillary MVS are mediated by different mechanisms, as already suggested previously.[20] Hence, the current study made two observations, which may directly affect our current understanding of the pathophysiology of SAH. DFX was applied systemically before SAH, in order to allow it to be present at high concentrations exactly at the site where the extravasated blood constricted subarachnoid vessels after SAH. This approach is ideal for a proof-of-principle study, however, does not allow a post-treatment protocol since DFX would not be able to reach the wall of subarachnoid vessels after the bleeding had already occurred. Therefore, iron chelation or inhibition of downstream mechanisms need to be addressed in future investigations using different approaches, e.g. flushing of the subarachnoid space with iron chelating solutions or systemic application of compounds inhibiting iron-induced cell death signaling.

It is increasingly recognized that pathophysiological events occurring within the first 72 hours after hemorrhage determine the extent of permanent brain injury after subarachnoid hemorrhage[5]. This phase, termed Early Brain Injury (EBI), is

characterized by severe microcirculatory dysfunction which leads to tissue ischemia and subsequent post-hemorrhagic brain damage[9, 22]. At later time points, i.e. later than 3-5 days after SAH, vasospasms of large pial arteries, typically diagnosed by angiography or transcranial Doppler sonography, occur in more than 40% of patients[23]. Both phenomena most probably contribute to the development of delayed cerebral ischemia (DCI) which is strongly associated with bad outcome after SAH[24]. We previously demonstrated that micro arterial constrictions, so-called microvasospasms (MVS), play a role in the development of microvascular dysfunction after SAH.[9, 19, 20]

According to the Hagen-Poiseuille equation, volume flow (volume derived according to time) is directly proportional to the pressure difference and to the 4th power of the inner radius. Therefore, a reduction of the vessel diameter of 15% (i.e. a reduction of the radius by 7.5%) results in a flow reduction of ~37%. With a CBF of ~60 (mL/100 g x min) this effect alone would relevantly reduce the CBF to ~38 mL/100 g x min. In combination with possibly compromised cerebral blood flow (due to intracranial hypertension, brain edema formation, microthrombosis etc.) the impairment of cerebral perfusion could be even more pronounced.

As of now, the mechanisms of post-hemorrhagic MVS formation are far from being understood thereby impeding the development of specific therapeutic interventions.

It was previously shown experimentally that NO application reverses micro arteriolar constriction,[25] improves CBF[26], and reduces the number of MVS by more than 80%. As a result, brain damage and functional outcome improved.[14, 27] These findings suggest that NO depletion early after SAH may play an important role for the development of microvasospasm formation and the subsequent functional outcome after SAH. In the early phase after hemorrhage, vessels of the pial microcirculation are covered with subarachnoid blood that spreads within the perivascular space of the middle cerebral artery. Blood breakdown products including hemoglobin, bilirubin, bilirubin oxidation products, and free as well as bound iron have previously been shown to play a role in delayed vasoconstriction after SAH, however, whether iron is also involved in early vasoconstriction remained unknown.[28, 29] This is quite surprising, since hemolysis occurs relatively early after SAH as demonstrated by the detection of free iron (Fe^{3+}) in cerebrospinal fluid of patients already within the first 24 hours after SAH, a time point where delayed spasms of large pial arteries are usually not present.[30, 31]

DFX is a water-soluble iron chelator which is used clinically to treat iron overload. The effect of DFX has been extensively studied in experimental models of intraventricular and intracerebral hemorrhage. In these models DFX reduced brain damage and hydrocephalus and showed neuroprotective properties.[32, 33] In patients, DFX applied after intracerebral hemorrhage reduced brain edema

formation.[34] In SAH, DFX application yielded mixed results with regard to its ability to reduce vasospasm of circle of Willis vessels, most likely due to the fact that it may not have reached the target area.[35] In experimental SAH DFX reduced brain iron overload, blood brain barrier impairment, and neuronal cell death and improved outcome.[36, 37] [17, 38] While some studies demonstrating positive effects of DFX explicitly looked at parameters of early brain injury,[17, 37] DFX effects on the cerebral microcirculation were never assessed as a possible cause for the observed neuroprotection. Hence, the present study demonstrates for the first time that the main protective effect of DFX may be mediated by a direct vascular effect, i.e. by reduction of the number of arteriolar microvasospasms. Because this protective effect was almost exclusively observed in microvessels covered with perivascular blood, we conclude that iron toxicity plays a causal role for the formation of MVS. The underlying mechanism are most probably the interruption of iron redox cycling leading to a reduction of reactive oxygen species formation in the vessel wall and a subsequent preservation of NO activity.[39]

Interestingly, the effect of DFX was only observed in pial arterioles with a diameter larger than 30 µm, i.e. those vessels which come into direct contact with significant amounts of blood. This observation suggests that iron-mediated vasoconstriction is only relevant in one compartment of the microvascular tree. This observation is further supported by the fact that despite reduction of the total number of MVS, total perfused vessel volume as a surrogate parameter for

parenchymal perfusion was not altered by DFX pretreatment since dilating only distal vessels is not sufficient to improve tissue perfusion.

DFX has been described to have a higher pharmacological affinity for Fe^{3+} than for Fe^{2+}.[40] Increased Fe^{3+} levels has been detected in SAH patients early after hemorrhage,[30, 31] while Fe^{2+} containing oxyhemoglobin seems to be involved in the pathophysiology of delayed vasospasm, occurring at later stages after SAH.[41] The role and the significance of Fe^{2+} vs. Fe^{3+} in early microcirculatory dysfunction or MVS is unclear, however, the higher affinity of DFX for Fe^{3+} could be an indication that it is the main effector of the effect seen in the present study. In the context of delayed spasms of large cerebral arteries, a Fe^{2+} chelating agent, 2,2-dipyridyl, showed better results than DFX,[42] therefore, a combination with a chelator of Fe^{2+}, e.g. may yield better results than DFX alone. Furthermore, DFX not only scavenges Fe^{3+} but has been recently shown to also inhibit Hypoxia-induced-factor prolyl hydroxylases (HIF PHD).[43] HIF PHD inactivation is neuroprotective after ischemic stroke[44] and intraparenchymal hemorrhage,[45] its (role in early brain injury after) SAH, however, is so far unknown. Further studies using selective HIF PHD inhibitors will be needed to differentiate between iron chelating and possible HIF PHD inhibiting effects of DFX. Currently, we cannot exclude that the effects observed may be partially due to HIF inactivation.

In conclusion, the results of the current study demonstrate that iron is a major mediator of early microvasospasm formation in large pial arterioles (diameter >30

μm) after SAH. Smaller arterioles were not affected suggesting that the mechanisms of microvasospasm formation differ between small and large pial arterioles, a phenomenon recently suggested by us in another context.[20] Since DFX dilated only the distal part of the microvascular tree, tissue perfusion was not improved.

Therefore, further studies are needed to identify the mechanisms underlying microvasospasm formation after subarachnoid hemorrhage in the whole microvascular tree and to assess whether iron chelation (by DFX or other chelating agents) may be a suitable therapeutic approach to treat early microvascular dysfunction after SAH.

Figure Legends

Figure 1

SAH induction and experimental design

A. Image of a mouse brain immediately after SAH removed following transcardial perfusion with saline, i.e. only extra- and perivascular blood is visible. The hematoma at the perforation site is indicated by a white arrow. This SAH model resulted in a blood distribution comparable to aneurysmal SAH in humans. **B**. Deep tissue penetrating 2-photon imaging was used to analyze the pial and the intraparenchymal cerebral microcirculation after SAH. Vessels were visualized with the plasma dye FITC dextran (**left**) after thinning of the scull above four different regions of interest (ROI; **right**). ROIs were placed over the territory of the middle cerebral artery. **C**. Deferoxamine or vehicle were injected i.v. 1.5 hours prior to SAH. SAH was induced under monitoring of intracranial pressure (ICP) and local cerebral blood flow (CBF). After a wake up period of 100 minutes, mice were re-anesthetized and *in vivo* 2-photon microscopy (IVM) of cerebral vessels was performed.

Figure 2

Multi-modal monitoring during SAH surgery

A. Continuous measurement of intracranial pressure (ICP) and **B**. cerebral blood flow (CBF) before and after SAH (time 0) in mice. ICP increased sharply and CBF dropped significantly after SAH. There was no difference between groups.

Figure 3

***In vivo* 2-photon microscopy of cerebral microvessels after SAH and after DFX or vehicle treatment**

A. 3D reconstruction of cerebral microvessels (green) and extravasated blood (red) after SAH. Blood distributes along cerebral microvessels thereby demonstrating 1) the perivascular spreading of blood/plasma after SAH and 2) the delivery of DFX to the cerebral microcirculation. **B**. A large pial arteriole after SAH and vehicle (**left**) or DFX treatment (**right**). Multiple, pearl-string like microvasospasms were identified after vehicle treatment, while no spams were present in a similar vessel after DFX treatment. Scale bar = 100 µm.

Figure 4

Quantification of the effect of Deferoxamine (DFX) after SAH

A. DFX significantly reduces the total number of vasospasms in all investigated vessels after SAH. This effect is exclusively observed in vessel segments covered with blood. **B**. Degree of microvasospasms in vessel categorized by size. All vessel categories were affected by constrictions up to 40% with a tendency of less severe spams towards larger vessels. DFX treatment abolished microvasospasms in arterioles with diameters ≥ 30µm. * $p < 0.05$.

Figure 5

Microvascular blood flow velocity and vessel density after SAH and DFX treatment

A. Blood flow velocity in arterioles and capillaries after SAH with (open bars) and without (closed bars) DFX treatment. As compared to values in the healthy brain (dotted lines)[46], blood flow velocity was reduced in all investigated vessel segments after SAH. There was not difference between treatment groups. **B**. The perfused vessel volume was also not different between groups, suggesting that despite preventing arteriolar microvasospasm DFX treatment did not improve microcirculatory failure after SAH since it did not prevent capillary constrictions.

Abbreviations

Animal Research: Reporting of In Vivo Experiments: ARRIVE; Cerebral blood flow: CBF; Deferoxamine: DFX; Early brain injury: EBI; Iron: Fe; Figure: Fig; Fluorescein isothiocyanate: FITC; Intracranial pressure: ICP; Middle cerebral artery: MCA; Microvasospasm: MVS; Nitric oxide: NO; Regions of interest: ROI; Subarachnoid hemorrhage: SAH; Table: Tab;

Conflicts of Interest

The authors declare that they have no financial or other conflicts of interest.

Acknowledgments

We would like to thank Uta Mamrak for excellent technical and organizational support.

Funding Sources

This work was funded by the Deutsche Forschungsgemeinschaft (DFG, German Research Foundation) under Germany's Excellence Strategy within the framework of the Munich Cluster for Systems Neurology (EXC 2145 SyNergy – ID 390857198) and by an individual DFG grant to NP (No. SCHO1385/1-1).

Supplementary Materials

Expanded statistical data

Table 1

	Vehicle (n=8)		Deferoxamine (n=8)	
	Mean ± SD		Mean ± SD	
	SAH induction	**Imaging**	**SAH induction**	**Imaging**
Temperature (°C)	37.1 ± 0.1	37.1 ± 0.1	37.1 ± 0.1	37.1 ± 0.1
End tidal pCO_2 (mmHg)	21.1 ± 0.5	20.2 ± 0.7	21.1 ± 1.0	19.9 ± 0.7
SpO_2 (%)	94 ± 2	96% ± 1%	93 ± 2	96% ± 3%
Respiratory Rate (n/min)	145 ± 7	142 ± 7	144 ± 3	141 ± 8
Heart Rate (n/min)	260 ± 23		353 ± 13**	
MAP (mmHg)		73 ± 6		67 ± 7
pH		7.27 ± 0.03		7.26 ± 0.03
pCO_2 (mmHg)		44.2 ± 3.8		42.3 ± 6.8
pO_2 (mmHg)		95.7 ± 13.8		101.4 ± 18.9

** $p<0.01$

References

1. Stienen MN, Germans M, Burkhardt JK, et al. Predictors of In-Hospital Death After Aneurysmal Subarachnoid Hemorrhage: Analysis of a Nationwide Database (Swiss SOS [Swiss Study on Aneurysmal Subarachnoid Hemorrhage]). *Stroke* 2018; 49: 333-340. 2018/01/18. DOI: 10.1161/strokeaha.117.019328.

2. Skrifvars MB and Parr MJ. Incidence, predisposing factors, management and survival following cardiac arrest due to subarachnoid haemorrhage: a review of the literature. *Scandinavian journal of trauma, resuscitation and emergency medicine* 2012; 20: 75. 2012/11/16. DOI: 10.1186/1757-7241-20-75.

3. Schubert GA, Seiz M, Hegewald AA, et al. Hypoperfusion in the acute phase of subarachnoid hemorrhage. *Acta neurochirurgica Supplement* 2011; 110: 35-38. 2010/12/01. DOI: 10.1007/978-3-7091-0353-1_6.

4. Honda M, Sase S, Yokota K, et al. Early cerebral circulatory disturbance in patients suffering subarachnoid hemorrhage prior to the delayed cerebral vasospasm stage: xenon computed tomography and perfusion computed tomography study. *Neurol Med Chir (Tokyo)* 2012; 52: 488-494. 2012/08/02. DOI: 10.2176/nmc.52.488.

5. Sehba FA, Hou J, Pluta RM, et al. The importance of early brain injury after subarachnoid hemorrhage. *Progress in neurobiology* 2012; 97: 14-37. 2012/03/15. DOI: 10.1016/j.pneurobio.2012.02.003.

6. Cahill J, Calvert JW and Zhang JH. Mechanisms of early brain injury after subarachnoid hemorrhage. *J Cereb Blood Flow Metab* 2006; 26: 1341-1353. 2006/02/17. DOI: 10.1038/sj.jcbfm.9600283.

7. Macdonald RL, Higashida RT, Keller E, et al. Clazosentan, an endothelin receptor antagonist, in patients with aneurysmal subarachnoid haemorrhage undergoing surgical clipping: a randomised, double-blind, placebo-controlled phase 3 trial (CONSCIOUS-2). *Lancet Neurol* 2011; 10: 618-625. 2011/06/07. DOI: 10.1016/S1474-4422(11)70108-9.

8. Schubert GA, Seiz M, Hegewald AA, et al. Acute hypoperfusion immediately after subarachnoid hemorrhage: a xenon contrast-enhanced CT study. *J Neurotrauma* 2009; 26: 2225-2231. 2009/11/26. DOI: 10.1089/neu.2009.0924.

9. Friedrich B, Muller F, Feiler S, et al. Experimental subarachnoid hemorrhage causes early and long-lasting microarterial constriction and microthrombosis: an in-vivo microscopy study. *J Cereb Blood Flow Metab* 2012; 32: 447-455. 2011/12/08. DOI: 10.1038/jcbfm.2011.154.

10. Sehba FA and Friedrich V. Early micro vascular changes after subarachnoid hemorrhage. *Acta neurochirurgica Supplement* 2011; 110: 49-55. 2010/12/01. DOI: 10.1007/978-3-7091-0353-1_9.

11. Uhl E, Lehmberg J, Steiger HJ, et al. Intraoperative detection of early microvasospasm in patients with subarachnoid hemorrhage by using orthogonal polarization spectral imaging. *Neurosurgery* 2003; 52: 1307-1315; disacussion 1315-1307. 2003/05/24.

12. Pennings FA, Bouma GJ and Ince C. Direct observation of the human cerebral microcirculation during aneurysm surgery reveals increased arteriolar contractility. *Stroke* 2004; 35: 1284-1288. 2004/04/17. DOI: 10.1161/01.STR.0000126039.91400.cb.

13. Clower BR, Yamamoto Y, Cain L, et al. Endothelial injury following experimental subarachnoid hemorrhage in rats: effects on brain blood flow. *Anat Rec* 1994; 240: 104-114. 1994/09/01. DOI: 10.1002/ar.1092400110.

14. Terpolilli NA, Feiler S, Dienel A, et al. Nitric oxide inhalation reduces brain damage, prevents mortality, and improves neurological outcome after subarachnoid hemorrhage by resolving early pial microvasospasms. *J Cereb Blood Flow Metab* 2016; 36: 2096-2107. 2015/12/15. DOI: 10.1177/0271678X15605848.

15. Chan PH. Reactive oxygen radicals in signaling and damage in the ischemic brain. *J Cereb Blood Flow Metab* 2001; 21: 2-14. 2001/01/10. DOI: 10.1097/00004647-200101000-00002.

16. Garton T, Keep RF, Hua Y, et al. Brain iron overload following intracranial haemorrhage. *Stroke Vasc Neurol* 2016; 1: 172-184. 2017/09/30. DOI: 10.1136/svn-2016-000042.

17. Lee JY, Keep RF, He Y, et al. Hemoglobin and iron handling in brain after subarachnoid hemorrhage and the effect of deferoxamine on early brain injury. *J Cereb Blood Flow Metab* 2010; 30: 1793-1803. 2010/08/26. DOI: 10.1038/jcbfm.2010.137.

18. Kilkenny C, Browne WJ, Cuthill IC, et al. Improving bioscience research reporting: the ARRIVE guidelines for reporting animal research. *PLoS Biol* 2010; 8: e1000412. 2010/07/09. DOI: 10.1371/journal.pbio.1000412.

19. Feiler S, Friedrich B, Scholler K, et al. Standardized induction of subarachnoid hemorrhage in mice by intracranial pressure monitoring. *J Neurosci Methods* 2010; 190: 164-170. 2010/05/12. DOI: 10.1016/j.jneumeth.2010.05.005.

20. Liu H, Dienel A, Scholler K, et al. Microvasospasms After Experimental Subarachnoid Hemorrhage Do Not Depend on Endothelin A Receptors. *Stroke* 2018; 49: 693-699. 2018/02/14. DOI: 10.1161/STROKEAHA.117.020028.

21. Anzabi M, Angleys H, Aamand R, et al. Capillary flow disturbances after experimental subarachnoid hemorrhage: A contributor to delayed cerebral ischemia? *Microcirculation* 2019; 26: e12516. 2018/11/16. DOI: 10.1111/micc.12516.

22. Terpolilli NA, Brem C, Buhler D, et al. Are We Barking Up the Wrong Vessels? Cerebral Microcirculation After Subarachnoid Hemorrhage. *Stroke* 2015; 46: 3014-3019. 2015/07/15. DOI: 10.1161/STROKEAHA.115.006353.

23. Stornelli SA and French JD. Subarachnoid Hemorrhage--Factors in Prognosis and Management. *J Neurosurg* 1964; 21: 769-780. 1964/09/01. DOI: 10.3171/jns.1964.21.9.0769.

24. Connolly ES, Jr., Rabinstein AA, Carhuapoma JR, et al. Guidelines for the management of aneurysmal subarachnoid hemorrhage: a guideline for healthcare professionals from the American Heart Association/american Stroke Association. *Stroke* 2012; 43: 1711-1737. 2012/05/05. DOI: 10.1161/STR.0b013e3182587839.

25. Sehba FA, Ding WH, Chereshnev I, et al. Effects of S-nitrosoglutathione on acute vasoconstriction and glutamate release after subarachnoid hemorrhage. *Stroke* 1999; 30: 1955-1961. 1999/09/02. DOI: 10.1161/01.str.30.9.1955.

26. Lilla N, Hartmann J, Koehler S, et al. Early NO-donor treatment improves acute perfusion deficit and brain damage after experimental subarachnoid hemorrhage in rats. *J Neurol Sci* 2016; 370: 312-319. 2016/10/25. DOI: 10.1016/j.jns.2016.09.032.

27. Agrawal A, Patir R, Kato Y, et al. Role of intraventricular sodium nitroprusside in vasospasm secondary to aneurysmal subarachnoid haemorrhage: a 5-year prospective study with review of the literature. *Minim Invasive Neurosurg* 2009; 52: 5-8. 2009/02/28. DOI: 10.1055/s-0028-1085454.

28. Clark JF and Sharp FR. Bilirubin oxidation products (BOXes) and their role in cerebral vasospasm after subarachnoid hemorrhage. *J Cereb Blood Flow Metab* 2006; 26: 1223-1233. 2006/02/10. DOI: 10.1038/sj.jcbfm.9600280.

29. Hugelshofer M, Buzzi RM, Schaer CA, et al. Haptoglobin administration into the subarachnoid space prevents hemoglobin-induced cerebral vasospasm. *J Clin Invest* 2019; 129: 5219-5235. 2019/08/28. DOI: 10.1172/JCI130630.

30. Gomes JA, Selim M, Cotleur A, et al. Brain iron metabolism and brain injury following subarachnoid hemorrhage: iCeFISH-pilot (CSF iron in SAH). *Neurocritical care* 2014; 21: 285-293. 2014/04/09. DOI: 10.1007/s12028-014-9977-8.

31. Suzuki H, Muramatsu M, Tanaka K, et al. Cerebrospinal fluid ferritin in chronic hydrocephalus after aneurysmal subarachnoid hemorrhage. *J Neurol* 2006; 253: 1170-1176. 2006/05/02. DOI: 10.1007/s00415-006-0184-1.

32. Meng H, Li F, Hu R, et al. Deferoxamine alleviates chronic hydrocephalus after intraventricular hemorrhage through iron chelation and Wnt1/Wnt3a inhibition. *Brain Res* 2015; 1602: 44-52. 2014/08/26. DOI: 10.1016/j.brainres.2014.08.039.

33. Cui HJ, He HY, Yang AL, et al. Efficacy of deferoxamine in animal models of intracerebral hemorrhage: a systematic review and stratified meta-analysis. *PLoS One* 2015; 10: e0127256. 2015/05/23. DOI: 10.1371/journal.pone.0127256.

34. Hua Y, Keep RF, Hoff JT, et al. Deferoxamine therapy for intracerebral hemorrhage. *Acta neurochirurgica Supplement* 2008; 105: 3-6. 2008/12/11.

35. Vollmer DG, Hongo K, Ogawa H, et al. A study of the effectiveness of the iron-chelating agent deferoxamine as vasospasm prophylaxis in a rabbit model of subarachnoid hemorrhage. *Neurosurgery* 1991; 28: 27-32. 1991/01/01.

36. Qin Y, Li G, Sun Z, et al. Comparison of the effects of nimodipine and deferoxamine on brain injury in rat with subarachnoid hemorrhage. *Behav Brain Res* 2019; 367: 194-200. 2019/04/07. DOI: 10.1016/j.bbr.2019.04.004.

37. LeBlanc RH, 3rd, Chen R, Selim MH, et al. Heme oxygenase-1-mediated neuroprotection in subarachnoid hemorrhage via intracerebroventricular deferoxamine. *J Neuroinflammation* 2016; 13: 244. 2016/09/14. DOI: 10.1186/s12974-016-0709-1.

38. Li Y, Yang H, Ni W, et al. Effects of deferoxamine on blood-brain barrier disruption after subarachnoid hemorrhage. *PLoS One* 2017; 12: e0172784. 2017/03/02. DOI: 10.1371/journal.pone.0172784.

39. Valko M, Leibfritz D, Moncol J, et al. Free radicals and antioxidants in normal physiological functions and human disease. *Int J Biochem Cell Biol* 2007; 39: 44-84. 2006/09/19. DOI: 10.1016/j.biocel.2006.07.001.

40. Gutteridge JM, Richmond R and Halliwell B. Inhibition of the iron-catalysed formation of hydroxyl radicals from superoxide and of lipid peroxidation by desferrioxamine. *Biochem J* 1979; 184: 469-472. 1979/11/15. DOI: 10.1042/bj1840469.

41. Macdonald RL and Weir BK. A review of hemoglobin and the pathogenesis of cerebral vasospasm. *Stroke* 1991; 22: 971-982. 1991/08/01.

42. Horky LL, Pluta RM, Boock RJ, et al. Role of ferrous iron chelator 2,2'-dipyridyl in preventing delayed vasospasm in a primate model of subarachnoid hemorrhage. *J Neurosurg* 1998; 88: 298-303. 1998/02/06. DOI: 10.3171/jns.1998.88.2.0298.

43. Speer RE, Karuppagounder SS, Basso M, et al. Hypoxia-inducible factor prolyl hydroxylases as targets for neuroprotection by "antioxidant" metal chelators: From ferroptosis to stroke. *Free Radic Biol Med* 2013; 62: 26-36. 2013/02/05. DOI: 10.1016/j.freeradbiomed.2013.01.026.

44. Karuppagounder SS and Ratan RR. Hypoxia-inducible factor prolyl hydroxylase inhibition: robust new target or another big bust for stroke therapeutics? *J Cereb Blood Flow Metab* 2012; 32: 1347-1361. 2012/03/15. DOI: 10.1038/jcbfm.2012.28.

45. Karuppagounder SS, Alim I, Khim SJ, et al. Therapeutic targeting of oxygen-sensing prolyl hydroxylases abrogates ATF4-dependent neuronal death and improves outcomes after brain hemorrhage in several rodent models. *Sci Transl Med* 2016; 8: 328ra329. 2016/03/05. DOI: 10.1126/scitranslmed.aac6008.

46. Chaigneau E, Roche M and Charpak S. Unbiased Analysis Method for Measurement of Red Blood Cell Size and Velocity With Laser Scanning Microscopy. *Front Neurosci* 2019; 13: 644. 2019/07/19. DOI: 10.3389/fnins.2019.00644.

Figure 1

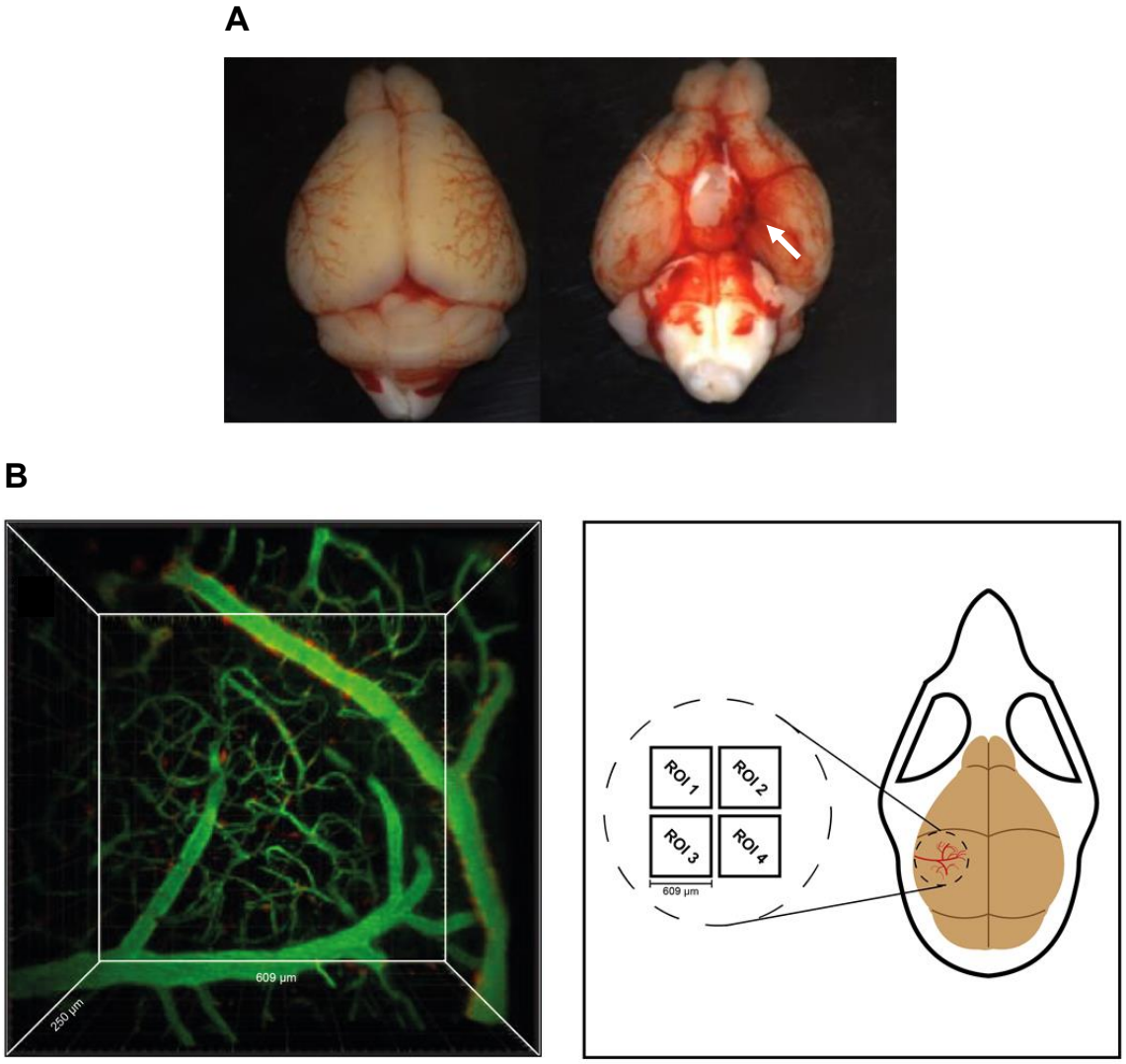
A
B
609 µm
250 µm
ROI 1
ROI 2
ROI 3
ROI 4
609 µm
C
Deferoxamine/
vehicle i.v
SAH induction
MCA perforation
surgical preparation
ICP, CBF
monitoring
awake period
surgical
preparation
IVM
time
-1.5h
0
20 min
2h
3h

Figure 2

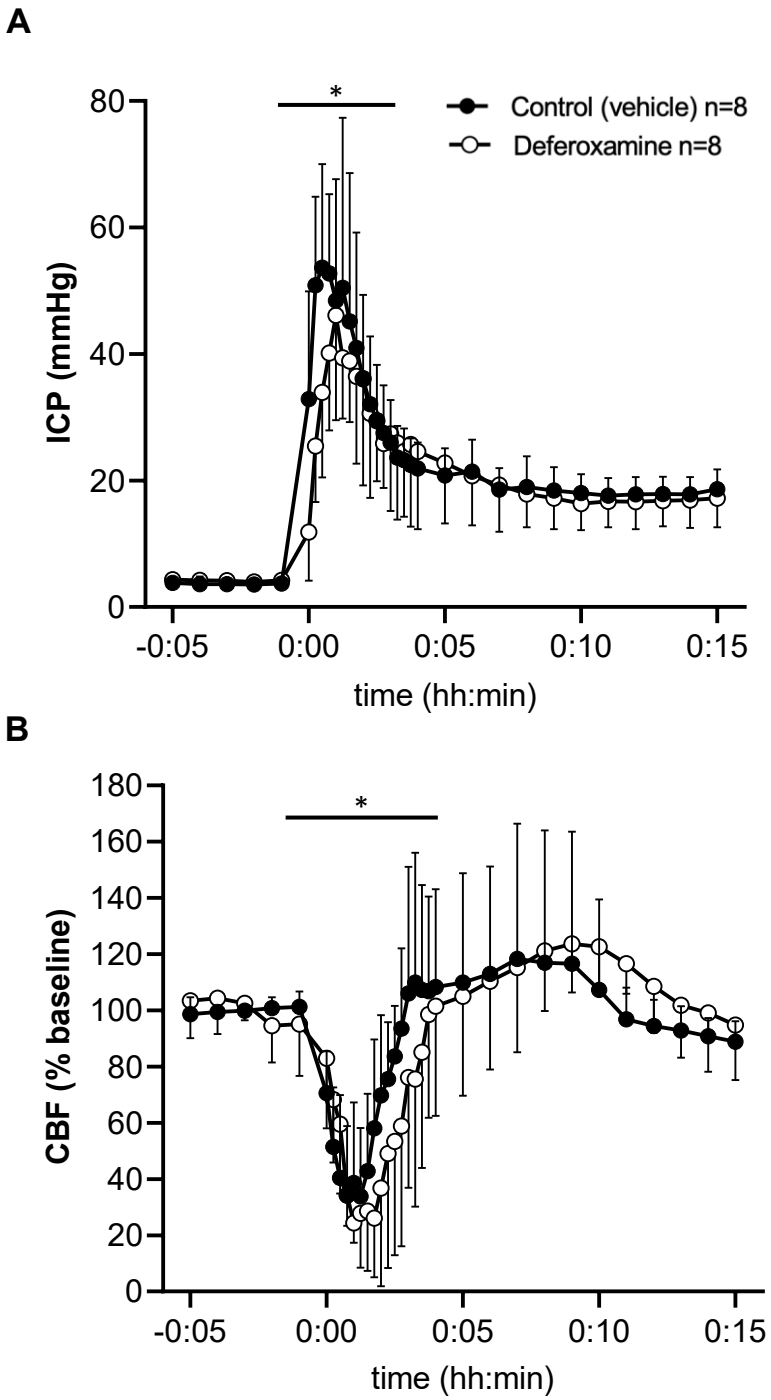
A
*
Control (vehicle) n=8
Deferoxamine n=8
ICP (mmHg)
80
60
40
20
0
-0:05
0:00
0:05
0:10
0:15
time (hh:min)
B
*
CBF (% baseline)
180
160
140
120
100
80
60
40
20
0
-0:05
0:00
0:05
0:10
0:15
time (hh:min)

Figure 3

A

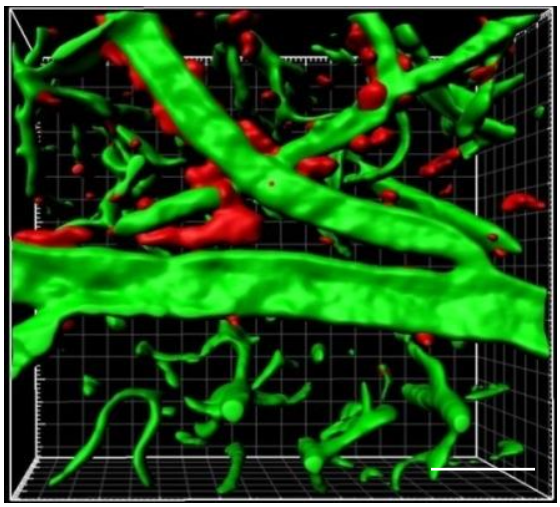

B

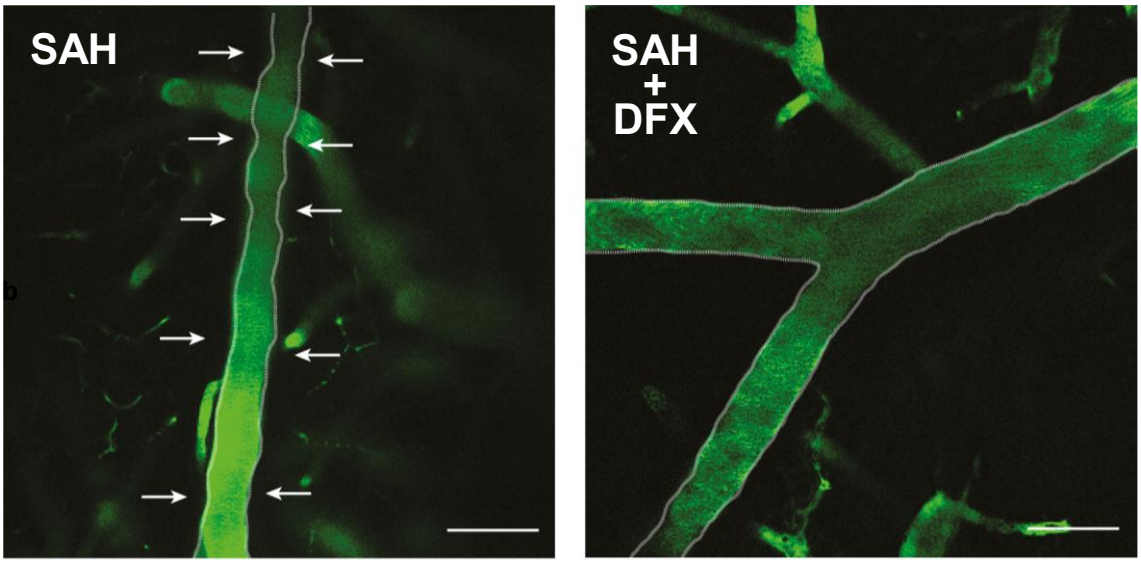

Figure 4

A

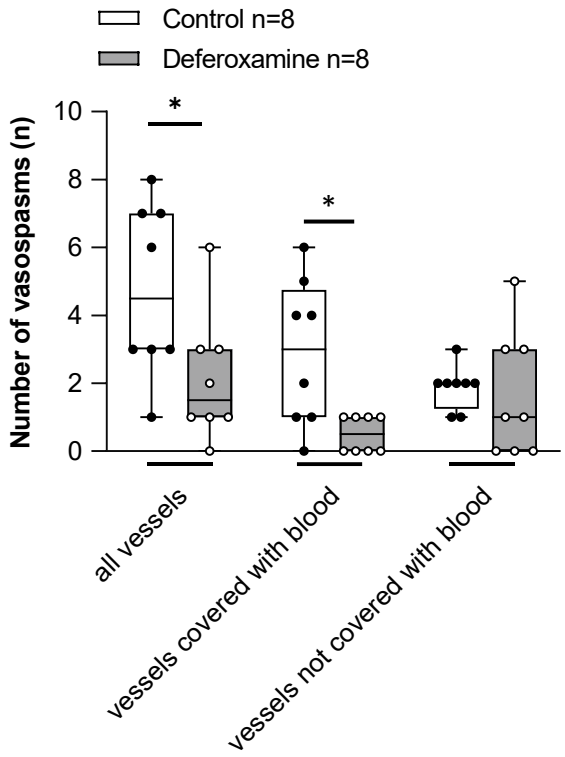
Control n=8
Deferoxamine n=8
Number of vasospasms (n)
10
8
6
4
2
0
*
*
all vessels
vessels covered with blood
vessels not covered with blood

B

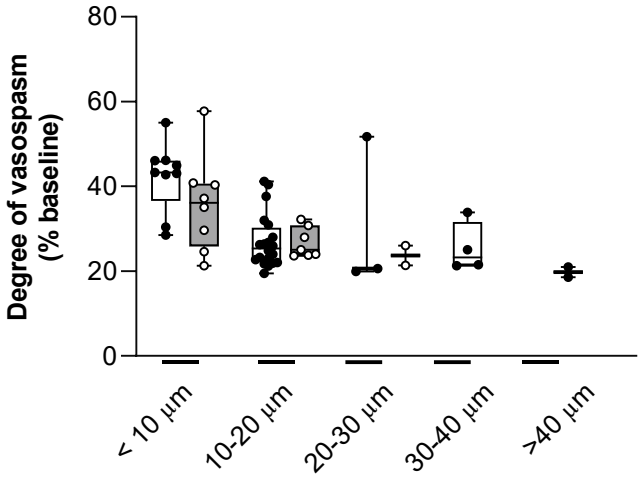
Degree of vasospasm (% baseline)
80
60
40
20
0
< 10 µm
10-20 µm
20-30 µm
30-40 µm
>40 µm

Figure 5

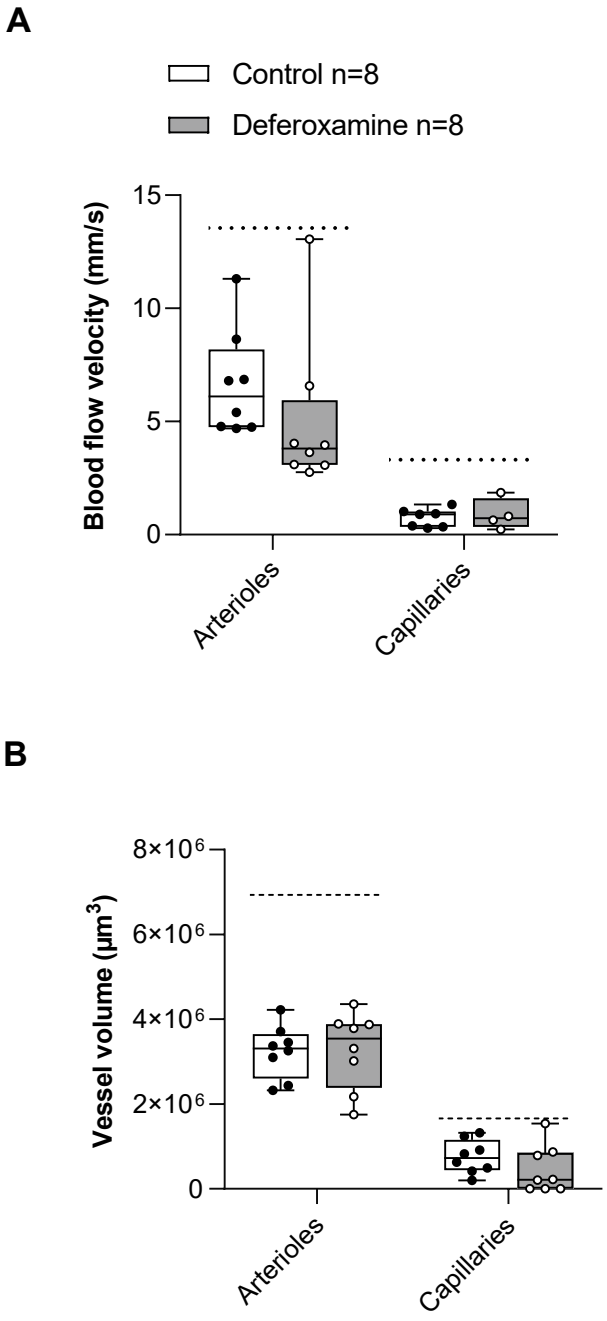
A
Control n=8
Deferoxamine n=8
Blood flow velocity (mm/s)
15
10
5
0
Arterioles
Capillaries
B
Vessel volume (µm³)
8×10⁶
6×10⁶
4×10⁶
2×10⁶
0
Arterioles
Capillaries